Chapter 5

Numerical Model

In this chapter, we discuss some applied aspects of the numerical model implementation. First, we give a more precise statement of the problem from the computational point of view. Next, we investigate the sensitivity of the model with respect to the variation of material parameters as well as their adequate scope for the numerical simulation. Finally, the algorithmic implementation of the overall adaptive numerical scheme of the non-linear elastic multilevel finite element approach is presented.

5.1 Simplified Numerical Model of Facial Tissue

In this section, we resume all previous discussions about the adequate simplified model of deformable facial tissue for the ”long term” prediction of patient’s postoperative appearance.

Simplified constitutive model. Complex material properties such as plastic and viscoelastic phenomena generally observed in soft tissue experiments may be neglected if the deformation is small or is performed over a period of time that suffices for recovery processes in living organism. For the ”long term” prediction of facial tissue, a simplified constitutive model based on a piecewise, isotropic, quasi-incompressible, non-linear hyperelastic material description is assumed.

Pure displacement problem. The original problem consists in the computation of the deformation for an object being under the impact of static loads implicitly given by the prescribed boundary displacements. Besides the displacement, no further physical terms describing the ”physics” of the surgical impact are available. Thus, the most natural approach for the numerical modeling of such quasi-

geometric problem is to apply the so-called pure displacement FE discretization of the BVP (3.50) as described in Section 3.3.

5.2 Sensitivity Analysis and Parameter Estimation

The existing literature on the mechanical properties of human tissues is abundant, but relatively scarce when one looks for converged, exact, comprehensive and representative data. There is a large scatter and uncertainty in the material properties of human tissue, according to sex, age, size, etc. Furthermore, there may be large differences found in tissue properties within an individual at different parts of the body [54].

In our approach, each homogeneous and isotropic subdomain $\Omega_i \subset \Omega$ of a composite elastic solid occupying the domain Ω is characterized by the stiffness and the compressibility, which are described by two elastic constants, the Young modulus E_i and the Poisson ratio ν_i , respectively. Hence, we are concerned with the estimation of the valid scope for $(E,\, \nu)$.

Quasi-incompressible material. The Poisson ratio is theoretically ranged in $\nu \in [0, 0.5]$. It is generally agreed that the adequate range for modeling of water rich soft tissue is $\nu \in [0.4, 0.4(9)]$ [34, 44, 85, 90, 41]. However, the choice of the particular value for ν within this range has some far-reaching consequences for the type of the FE discretization approach. As we have mentioned above, the pure displacement FE discretization locks for "almost incompressible" materials $\nu \approx 0.5$. The value of $\nu = 0.45$ is considered as an admissible upper threshold for the pure displacement FE method. Materials with $\nu > 0.45$ have to be simulated with mixed finite elements, where the pressure $\mathbf{p}$ is treated as an independent variable in addition to the displacement $\mathbf{u}$. Since the non-elliptic mixed formulation is much more computationally expensive in comparison with the efficient pure displacement approach, the estimation of the quantitative difference between the quasi-incompressible $\nu = 0.45$ and incompressible $\nu = 0.5$ constitutive model is of a general interest.

Hence, we are going to estimate the modeling error in displacements corresponding to the Poisson ratio by studying the explicit dependence of some close form solution of elasticity theory on ν. For this purpose, we use the so-called *fundamental solution* of linear elasticity, see Appendix A. First, we write the norm of the displacement (A.2) in the following form

$$u = A(f, r)\, B(\nu, \alpha)\,, \tag{5.1}$$

where $u = |\mathbf{u}|$ and

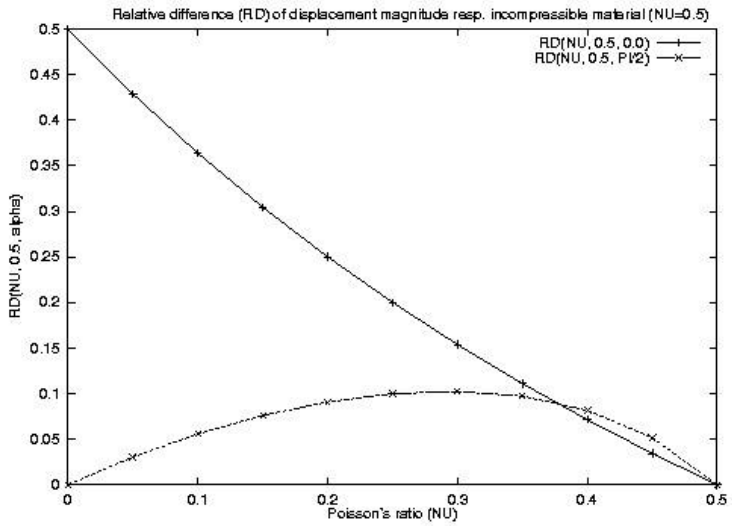

Figure 5.1: Relative difference of the displacements for a compressible ($\nu < 0.5$) and incompressible ($\nu = 0.5$) medium as a function of the Poisson ratio $RD_{||} = RD(\nu, 0.5, \alpha = 0),\ RD_{\perp} = RD(\nu, 0.5, \alpha = \frac{\pi}{2})$ (see explanations in text).

$$
\begin{aligned}
A(f, r) &= \frac{1}{8\pi\, E}\frac{f}{r}\,, \\
B(\nu, \alpha) &= \frac{1+\nu}{1-\nu}\sqrt{(3-4\nu)^2 + \cos^2\alpha\,(7-8\nu)}\,.
\end{aligned}
\tag{5.2}
$$

We are interested in the estimation of the relative difference $RD = \left|\frac{u(\nu_2)-u(\nu_1)}{u(\nu_1)}\right|$

$$
RD = \left|\frac{A\,B(\nu_2) - A\,B(\nu_1)}{A\,B(\nu_1)}\right| = \left|\frac{B(\nu_2) - B(\nu_1)}{B(\nu_1)}\right|\,. \tag{5.3}
$$

(5.3) shows that the relative difference is a function of three variables $RD = RD(\nu_1, \nu_2, \alpha)$ and does not depend on f, r and E. Since RD weakly depends on the angle to the vector of the acting force density $RD(\alpha) \sim |\cos\alpha|$, we observe two extreme cases, namely $RD_{||} = RD(\alpha = 0)$ and $RD_{\perp} = RD(\alpha = \frac{\pi}{2})$

$$
\begin{aligned}
RD_{||} &= RD(\nu_1 = 0.45, \nu_2 = 0.5, \alpha = 0) = 0.034483, \\
RD_{\perp} &= RD(\nu_1 = 0.45, \nu_2 = 0.5, \alpha = \tfrac{\pi}{2}) = 0.051724.
\end{aligned}
\tag{5.4}
$$

From (5.4), it follows that the relative difference of the displacements for a quasi-incompressible ($\nu = 0.45$) and incompressible ($\nu = 0.5$) material lie in the range between 3.4% and 5.2% in every point of the domain Ω occupied by a body. In Figure 5.1, $RD_{||} = RD(\nu, 0.5, 0)$ and $RD_{\perp} = RD(\nu, 0.5, \frac{\pi}{2})$ as functions of $\nu \in [0, 0.5]$ are plotted.

Table 5.1: Young modulus E of some soft tissues.

Tissue	E, MPa	Reference
Elastin	0.6	Fung 1993, [44]
Collagen	1×10^3	Fung 1993, [44]
Thoracic aorta	0.62	Duck 1991, [34]
Abdominal aorta	1.2	Duck 1991, [34]
Nasal cartiladge	5.6	Duck 1991, [34]
Muscle, along fibers	0.5	Duck 1991, [34]
Muscle, across fibers	0.79	Duck 1991, [34]
Brain	0.25	Simbio-d2a, [41]
Fat	5×10^{-3}	Samani 1999, [104]
Skin	0.5	Samani 1999, [104]
Fat	1×10^{-3}	Schnabel 2001, [108]
Skin	0.09	Schnabel 2001, [108]

Relative stiffness. In contrast to the Poisson ratio, the value of the positive Young modulus $E > 0$ describing the material stiffness is theoretically not limited by any constrains. The values of the Young modulus for soft tissue to be found in the literature underlie such heritable variations that the stiffness of a particular tissue usually cannot be estimated on the basis of existing data, see Table 5.1. Although some methods for in-vivo and in-vitro measurement of soft tissue properties are presented in the literature [37, 121, 81], no reliable approach is currently known which permits the derivation of individual material properties of facial tissues.

However, if the boundary conditions are given in the form of prescribed displacements, the knowledge of the *absolute material stiffness* is not necessarily required. Indeed, the resulting homogeneous system of equations $\mathbf{A}\,\mathbf{u} = \mathbf{0}$ is not sensitive with respect to the absolute value of the Young modulus (in $[Pascal]$), since it only makes sense, if the forces $\mathbf{f}$ (in $[Newton]$) on the right-hand side of the inhomogeneous system $\mathbf{A}\,\mathbf{u} = \mathbf{f}$ are given. The natural way to describe the stiffness within the quasi-geometrical formulation is to introduce the non-dimensional *relative stiffness*. Formally, this corresponds to scaling the homogeneous system with the stiffness of the reference material. Thus, the relative stiffness is defined as a ratio

$$rE_i = \frac{E_i}{E_0}\,,\ i = 0, 1, 2...\,, \tag{5.5}$$

Table 5.2: Absolute vs. relative stiffness.

material ID	absolute stiffness, E_i	relative stiffness, rE_i
0	E_0	1
1	E_1	E_1/E_0
2	E_2	E_2/E_0
3	E_3	E_3/E_0
...	...	...
n	E_n	E_n/E_0

where E_i is the absolute stiffness of the i-th material and E_0 is the absolute stiffness of the reference material. As long as no forces in $[Newton]$ are given, the absolute stiffness E_i can be replaced by rE_i. The first trivial consequence of (5.5) is that in the case of only one material (homogeneous domain) the choice of the Young modulus is practically irrelevant for the resulting deformation, since $rE_0 = E_0/E_0 = 1$. If the domain Ω consists of N subdomains $\Omega_i \subset \Omega$ (piecewise homogeneous domain) with E_i such that $E_i \neq E_j\ ,\ i \neq j$, merely $N-1$ unknown parameters rE_i are needed to describe such multi-composite material, see Table 5.2. If the domain of interest consists of only two tissue types, for example, muscle (M)and skin (S), merely one unknown parameter, namely, the ratio E_M/E_S has to be estimated.

Stiffness estimation from CT scans. In computer assisted surgery, patient's data are represented with the tomographic images. Since the grey scale value, especially, in the case of CT images correlates with the physical properties of scanned material, these data can be used for the estimation of the local tissue stiffness. The grey scale value (HU: Hounsfield unit) correlates to the density $HU \sim \rho$ and in turn the Young modulus is a function of the density [16, 1]

$$E(\rho) = A + B\rho^p\,, \tag{5.6}$$

where A, B and p are some real number constants. Thus, the implicit mapping $HU \rightarrow \rho \rightarrow E$ should be generally possible. In [74], such mapping $E(HU)$ in the form of a heuristic graph is proposed. However, there is no established derivation of the closed-form function $E(HU)$ or more detailed investigation of some heuristic relationships between E and HU for soft tissue.

5.3 Details of Implementation

In this section, we give an overview of some aspects of the computational implementation of our numerical model.

General software remarks. Finite element modeling and FE-based material engineering, in particular, is one of the oldest, but still the most extensive domains of computational physics and mathematics. The FEM incorporates a plethora of nested complex mathematical and programming technical problems, which makes the FEM software difficult to develop, to understand and to use. Indeed, modern FEM code has to provide

- flexible and efficient handling of arbitrary grids
- adaptive mesh refinement
- clear interface for physical problem definition, including
  - PDE operator discretization in appropriate functional space
  - constant parameter variation/control
  - type of numerical integration
  - type of problem solver
- efficient adaptive numerical techniques for assembling and solving the resulting system of equations based on error estimators
- user defined IO
- dynamic memory handling

The existing FEM packages do provide a useful user interface for FE analysis. However, most of them are extensive and expensive commercial software packages still requiring a lot of time to learn by ropes.

At the very beginning of this work, first linear elastic FE analysis has been performed with the help of *Kaskade* toolkit [36]. We developed the FEM code, which was used in further investigations presented in the next chapters. In what follows, the basic concept of this software is described.

The C source code (400 kB) comprises more than 200 routines and functions and is based on the following structures.

```
//-------------------------------------------------------------------

struct {
   double  x[3];        // node coordinates
   double  u[3];        // node displacement
   double  du[3];       // displacement increment
   double  f[3];        // nodal loads
   double  df[3];       // load increment
   int     nNbs;        // number of node neighbors
   int     *nb;         // array of node neighbors  nb[nNbs]
   double  *A;          // nodal stiffness  A[3*3*nNbs]
   int     nNbTd;       // number of neighbor tetrahedra
   int     *ndTd;       // array of neighbor tetrahedra  ndTd[nNbTd]
   int     nNbTr;       // number of neighbor triangles
   int     *ndTr;       // array of neighbor triangles  ndTr[nNbTr]
   int     nNbEd;       // number of neighbor edges
   int     *ndEd;       // array of neighbor edges  ndEd[nNbEd]
} meshNd;               //  mesh node

//-------------------------------------------------------------------

struct {
   int  edNode[2];      // edge nodes
   int  markerId;       // multipurpose marker Id
} meshEd;               //  mesh edge

//-------------------------------------------------------------------

struct {
   int     trNode[3];   // triangle nodes
   double  n[3];        // outer normal
   int     bId;         // boundary condition Id
   int     sId;         // surface type Id
} meshTr;               //  mesh triangle


//-------------------------------------------------------------------

struct {
   int  tdNode[4];      // tetrahedral nodes
   int  markerId;       // multipurpose marker Id
   int  mId;            // material type Id
} meshTd;               //  mesh tetrahedron
```

```
//-----------------------------------------

struct {
  int      nNds;     // number of nodes
  meshNd   *nd;      // array of nodes nd[nNodes]
  int      nEds;     // number of edges
  meshEd   *ed;      // array of edges ed[nEds]
  int      nTrs;     // number of triangles
  meshTr   *tr;      // array of triangles tr[nTrs]
  int      nTds;     // number of tetrahedra
  meshTd   *td;      // array of tetrahedra td[nTds]
  int      nSrs;     // number of surface patches
  int      *sr;      // array of surface patches sr[nSrs]
  int      nMts;     // number of materials
  int      *mt;      // array of materials mt[nMts]
  double   *EMOD;    // array of Young moduli EMOD[nMts]
  double   *NU;      // array of Poisson ratios NU[nMts]
} Mesh;

//-----------------------------------------
```

This is only a brief overview of the very basic structures. At present, dozens of attributes and parameters are required in our approach to describe composite facial tissue and to get a smart control on the FE computation of its deformation.

Adaptive algorithmic scheme. The overall algorithmic scheme for the adaptive calculation of non-linear elastic deformations is shown in Figure 5.2.

From our findings, the adaptivity of the numerical scheme on different levels of problem solving is essential for the achievement of the efficient and robust performance. The main adaptive features of our approach include

- adaptive mesh refinement,
- adaptive linear/non-linear assembly of stiffness matrix,
- adaptive solving scheme, incl. PCG, ordinary and simplified Newton-PCG.

Hardware platforms. The numerical model for soft tissue simulations is developed for the application in the clinical environment on comparatively low-cost hardware platforms. The computations presented in this work are performed on an SGI Onyx II with 195MHz as well as on PC Pentium PIII with 600MHz and 128MB RAM.

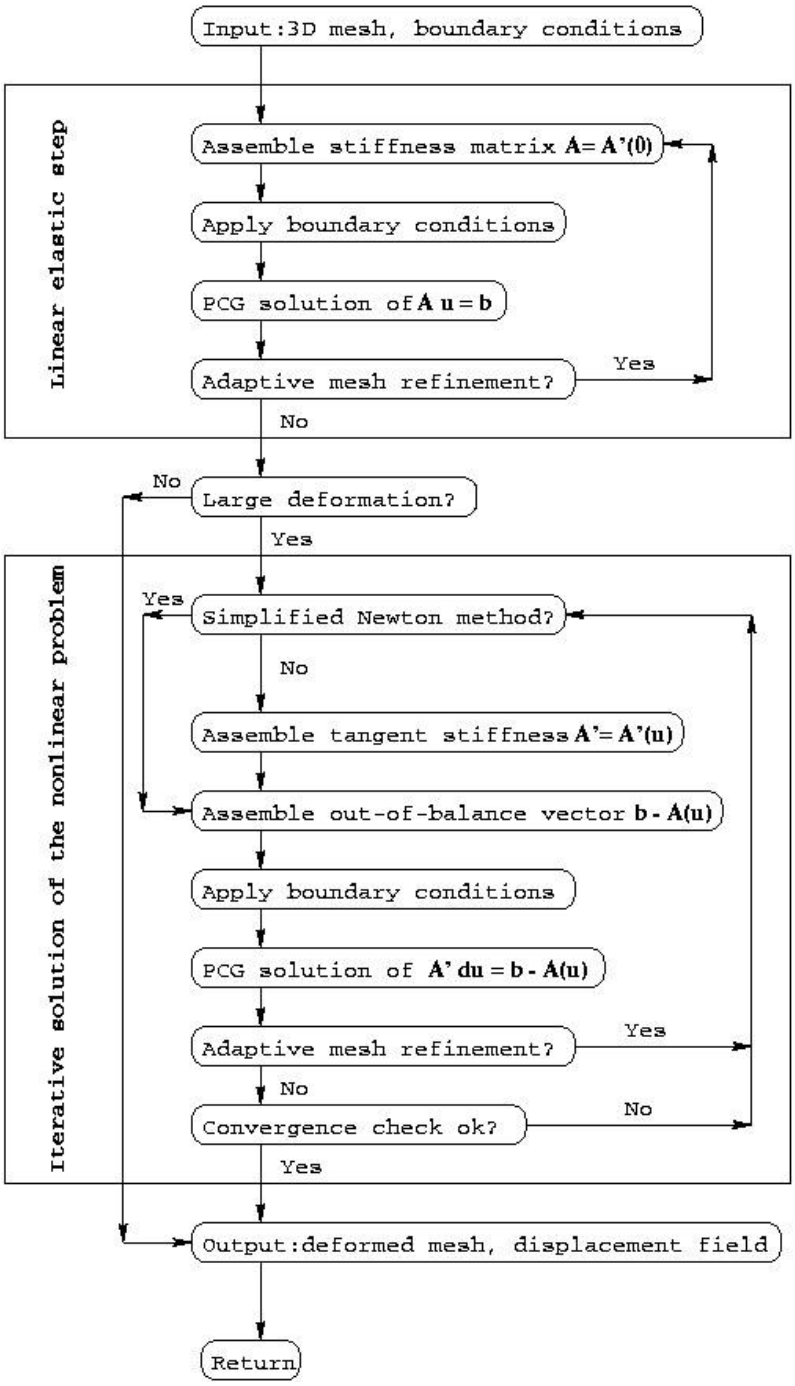

Figure 5.2: Overall algorithmic scheme.